Video Article

Preparing an Isotopically Pure ^{229}Th Ion Beam for Studies of ^{229m}Th

Lars von der Wense[1], Benedict Seiferle[1], Ines Amersdorffer[1], Peter G. Thirolf[1]

[1]Faculty of Physics, Ludwig-Maximilians-Universität München

Correspondence to: Lars von der Wense at L.Wense@physik.uni-muenchen.de

URL: https://www.jove.com/video/58516
DOI: doi:10.3791/58516

Keywords: Engineering, Issue 147, Nuclear clock, 229-Thorium isomer, buffer-gas cell, ion guide, Paul trap, mass separation, alpha decay, internal conversion

Date Published: 5/3/2019

Citation: Wense, L.v., Seiferle, B., Amersdorffer, I., Thirolf, P.G. Preparing an Isotopically Pure ^{229}Th Ion Beam for Studies of ^{229m}Th. *J. Vis. Exp.* (147), e58516, doi:10.3791/58516 (2019).

Abstract

A methodology is described to generate an isotopically pure ^{229}Th ion beam in the 2+ and 3+ charge states. This ion beam enables one to investigate the low-lying isomeric first excited state of ^{229}Th at an excitation energy of about 7.8(5) eV and a radiative lifetime of up to 10^4 seconds. The presented method allowed for a first direct identification of the decay of the thorium isomer, laying the foundations to study its decay properties as prerequisite for an optical control of this nuclear transition. High energy ^{229}Th ions are produced in the α decay of a radioactive ^{233}U source. The ions are thermalized in a buffer-gas stopping cell, extracted and subsequently an ion beam is formed. This ion beam is mass purified by a quadrupole-mass separator to generate a pure ion beam. In order to detect the isomeric decay, the ions are collected on the surface of a micro-channel plate detector, where electrons, as emitted in the internal conversion decay of the isomeric state, are observed.

Video Link

The video component of this article can be found at https://www.jove.com/video/58516/

Introduction

The first excited metastable state in the thorium-229 nucleus, denoted as ^{229m}Th, exhibits a special position in the nuclear landscape, as it possesses the lowest nuclear excitation energy of all presently known ca. 176,000 nuclear excited states. While typical nuclear energies range from keV up to the MeV region, ^{229m}Th possesses an energy of below 10 eV above the nuclear ground state[1,2,3]. The currently most accepted energy value for this state is 7.8(5) eV[4,5]. This low energy value has triggered interest from different physical communities and led to the proposal of several interesting applications. Among them are a nuclear laser[6], a highly stable qubit for quantum computing[7] and a nuclear clock[8,9].

The reason that ^{229m}Th is expected to offer a broad variety of applications is based on the fact that, due to its extraordinary low energy, it is the only nuclear state that could allow for direct nuclear laser excitation using currently available laser technology. So far, however, direct nuclear laser excitation of ^{229m}Th was prevented by insufficient knowledge of the metastable state's parameters like its precise energy and lifetime. Although the existence of a nuclear excited state of low energy in ^{229}Th was already conjectured in 1976[10], all knowledge about this state could only be inferred from indirect measurements, not allowing for a precise determination of its decay parameters. This situation has changed since 2016, when the first direct detection of the ^{229m}Th decay opened the door for a multitude of measurements aiming to pin down the excited state's parameters[11,12]. Here, a detailed protocol is provided, which describes the individual steps required for a direct detection of ^{229m}Th as achieved in the experiment of 2016. This direct detection provides the basis for a precise determination of the ^{229m}Th energy and lifetime and therefore for the development of a nuclear clock. In the following the concept of a nuclear clock as the most important application for ^{229m}Th will be discussed.

With a relative linewidth of $\Delta E/E \sim 10^{-20}$ the ground-state transition of the thorium isomer potentially qualifies as a nuclear frequency standard ('nuclear clock')[8,9]. Due to an atomic nucleus about 5 orders of magnitude smaller compared to the atomic shell, the nuclear moments (magnetic dipole and electric quadrupole) are accordingly smaller than the ones in atoms, rendering a nuclear clock largely immune against external perturbations (compared to the present state-of-the-art atomic clocks). Therefore, a nuclear frequency standard promises a highly stable and accurate clock operation. Although the accuracy achieved in the best present atomic clocks reaches about 2.1×10^{-18} [13], corresponding to a deviation of 1 second in a time period considerably longer than the age of the universe, nuclear clocks hold the potential of a further improvement which could become essential for a vast field of applications. Satellite-based navigational systems like the Global Positioning System (GPS), Global Navigation Satellite System (GLONASS) or Galileo presently operate with a positioning precision of a few meters. If this could be improved to the centimeter or even millimeter scale, a plethora of applications could be envisaged, from autonomous driving to freight or component tracking. Besides highly accurate clocks, such systems would require reliable uninterrupted operation, with long-term drift stability that secures long-resynchronization intervals. The use of nuclear clocks could turn out beneficial from this practical point of view. Further practical applications of (synchronized networks of) nuclear clocks could lie in the field of relativistic geodesy[14], where the clock acts as a 3D gravity sensor, relating local gravitational potential differences ΔU to measured (relative) clock frequency differences $\Delta f/f$ via the relation $\Delta f/f = -\Delta U/c^2$ (c denoting the speed of light). The best present clocks are capable of sensing gravitational shifts from height differences of about ±2 cm. Thus, ultra-precise measurements using a nuclear clock network could be used to monitor the dynamics of volcanic magma chambers or tectonic plate movements[15]. Moreover, the use of such clock networks was proposed as a tool to search for the theoretically

described class of topological dark matter[16]. Extensive discussion can be found in the literature on the application of a ^{229m}Th-based nuclear clock in the quest for the detection of potential temporal variations of fundamental constants like the fine structure constant α or the strong interaction parameter (m_q/Δ_{QCD}, with m_q representing the quark mass and Δ_{QCD} the scale parameter of the strong interaction), suggested in some theories unifying gravity with other interactions[17]. The detection of a temporal variation in the ground-state transition energy of ^{229m}Th may provide an enhanced sensitivity by about 2-5 orders of magnitude for temporal variations of the fine structure constant or the strong interaction parameter[18,19,20,21,22,23,24,25,26]. The current experimental limit for such a variation of α amounts to $(d\alpha/dt)/\alpha=-0.7(2.1)10^{-17}/yr$[27]. In the following the experimental approach for the direct detection of the ^{229m}Th ground-state decay will be described.

Evidence for the existence of the 229-thorium isomer until recently could only be inferred from indirect measurements, suggesting an excitation energy of 7.8(5) eV (equivalent to a wavelength in the vacuum ultra-violet spectral range of 160(11) nm)[4,5]. Our experimental approach, aiming at a direct identification of the isomeric ground-state deexcitation of the ^{229m}Th isomer, builds on a spatial separation of the isomer population in a buffer-gas stopping cell, followed by an extraction, and mass-separated transport towards a suitable detection unit to register the deexcitation products[28,29]. Thus population and deexcitation of the isomer can be disentangled, resulting in a clean measurement environment, unaffected by prompt background contributions. Population of the isomer is achieved via the α decay from a radioactive ^{233}U source, where a 2% decay branch proceeds not directly to the ground state of ^{229}Th, but populates the isomeric first excited state instead. α-decay recoil nuclei are thermalized in an ultra-pure helium atmosphere of a buffer-gas stopping cell, before being guided by electric radiofrequency (RF) and direct current (DC) fields towards an extraction nozzle, where the emerging supersonic gas jet drags them into an adjacent vacuum chamber, housing a (segmented) radiofrequency quadrupole (RFQ) structure acting as ion guide, phase-space cooler and potentially also as linear Paul trap for bunching the extracted ions. For a detailed description of the buffer-gas stopping cell and extraction RFQ see Refs.[30,31,32]. Since up to that moment the extracted ion beam contains in addition to $^{229(m)}$Th also the chain of α decay daughter products, mass separation is performed using a quadrupole mass separator (QMS) in a subsequent vacuum chamber to finally generate an isotopically pure $^{229(m)}$Th beam in selectable charge states (q=1-3). A detailed description of the QMS can be found in Refs.[33,34]. Detection of the isomeric decay was achieved by impinging the Th ions directly on the surface of a microchannel-plate detector (MCP), where electrons are liberated, accelerated towards a phosphor screen and viewed by a charge-coupled device (CCD) camera. An overview of the experimental setup is shown in **Figure 1**. A detailed description is given in Ref.[35].

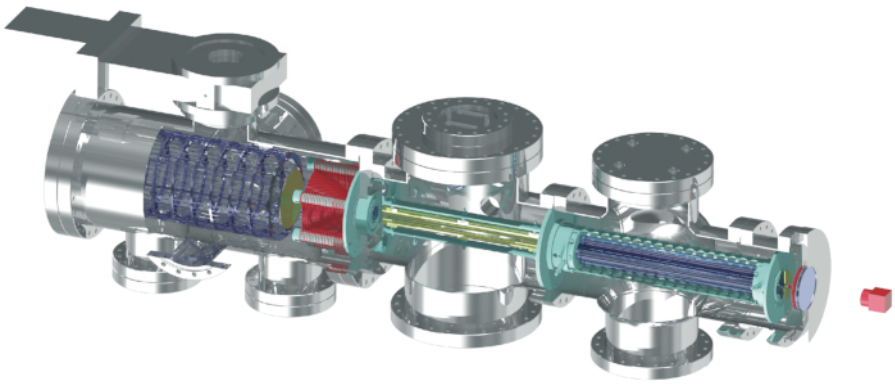

Figure 1: Overview of the experimental setup. The thorium-229 isomer is populated via the 2% decay branch in the α decay of uranium-233. ^{229m}Th ions, leaving the ^{233}U source due to their kinetic recoil energy, are thermalized in a buffer-gas stopping cell filled with 30 mbar helium gas. The ions are extracted from the stopping volume with the help for RF and DC fields and a low-energy ion beam is formed with the help of a radio-frequency quadrupole (RFQ). The ion beam is mass-purified with the help of a quadrupole-mass-separator (QMS) and the ions are softly implanted into the surface of a micro-channel-plate (MCP) detector combined with a phosphor screen which allows for spatially resolved detection of any occurring signals. With kind permission of Springer Research, this figure has been modified from[11]. Please click here to view a larger version of this figure.

The following protocol describes the underlying procedure to generate the $^{229(m)}$Th ion beam that enabled the first direct detection of the ground-state decay of the thorium isomer, thus laying the foundation for studying its decay properties as a prerequisite of the ultimately envisaged all-optical control of this exotic nuclear state towards its application as an ultra-precise nuclear frequency standard. For better orientation a schematic overview of the setup used for direct detection of the isomeric decay[11] is provided in **Figure 2**, containing a numerical labelling of the components addressed in the following protocol. Also the components used for lifetime determination[12] are contained as an inset.

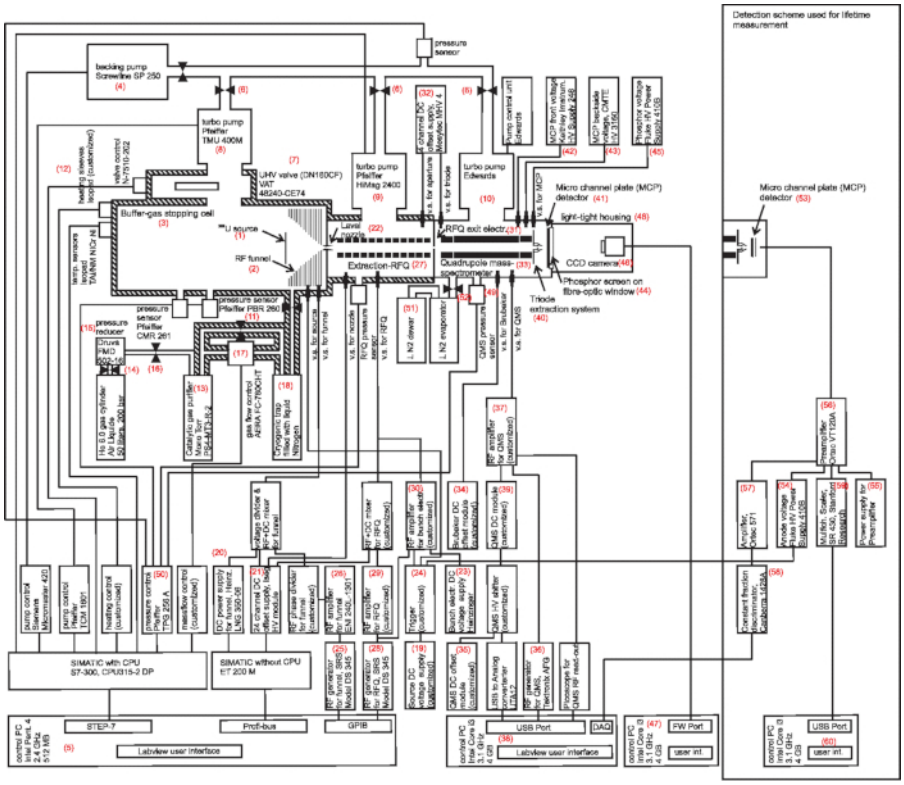

Figure 2: Schematic sketch of the experimental setup used for isomeric decay detection. The components used for lifetime measurement are shown as an inset. Individual components that will be referenced in the protocol section are numerically labelled. Please click here to view a larger version of this figure.

Protocol

Note: Numbers given in the Protocol will reference to Figure 2.

1. Direct Detection of Th-229 Isomeric Decay

1. Mounting of the 233-uranium source
    1. Mount the 233-uranium α source (1) through an access flange opening in the gas cell vacuum chamber to the upstream end of the funnel ring electrode system (2) inside the gas cell (3).
    NOTE: The 290 kBq, 90 mm diameter ^{233}U source was produced via molecular plating onto a titanium-sputtered Si wafer[36]. In order to achieve optimum α recoil-efficiency of the source, its thickness should not exceed 16 nm, being the stopping range of 84 keV ^{229}Th in uranium.
    2. Connect the cable to the source mount in order to allow for a DC offset of the source. Close and seal the access flange and connect the external wiring to the ^{233}U source.

2. **Evacuation of the vacuum chamber and bake out**
    1. Start evacuation of the complete vacuum system by starting the roughing vacuum pump (4) if shut down (controlled via a computer-based user interface (5)) and open the three (hand-operated) valves (6) that connect the individual parts of the differential pumping stages to the roughing pump.
    NOTE: Start opening the valves from chambers downstream of the gas cell with open gate valve (7) towards the turbo molecular pump of the gas cell to create a pressure gradient that prevents potential contaminations from downstream chambers to be sucked into the gas-cell chamber where highest cleanliness is demanded.
    2. Once the pressures have reached a level in the sub-mbar range (read out via user interface (5)) start the turbo pumps of the gas cell (8), the extraction radio-frequency quadrupole (RFQ) (9) and the quadrupole mass separator (QMS) (10).
    3. (optional) Open the bypass valve (11) to also allow for efficient evacuation of the gas-supply tubing.
    4. Continue pumping for a few (4-5) hours until reaching saturation pressure, typically in the range of low 10^{-7} mbar.
    5. Start the baking system (12) via the user interface (5) with an upramping (typically 20 °C - 40 °C per hour) heating curve to a maximum of 130 °C.
    6. Keep baking the vacuum system at 130 °C for 1-2 days until the pressure readings start to decrease.
    7. Start the cooling sequence of the baking system via the user interface (5) with a downramping sequence, typically 20 °C - 40 °C per hour.
    NOTE: Cooldown of the system typically requires 8 hours and is performed overnight. Successful preparation of the vacuum system is achieved when the final cell-pressure after cool down ranges below $5x10^{-10}$ mbar. The pressures in the RFQ and QMS chamber will be in the 10^{-9} mbar and 10^{-8} mbar range, respectively.

8. Connect the external wiring to the RFQ vacuum chamber.

3. **Preparation of the gas system and supply of ultra-pure He**
   1. Start the MonoTorr gas-purifier (13) and wait 20 minutes until it has reached its operating temperature.
   2. Close the bypass valve (11) if open.
   3. Open the He-gas cylinder (14) (He of 99.9999 % purity is used for operation).
   4. Open the pressure reducer valve (15) until a pressure of about 0.5 bar is shown.
   5. Open the valve that connects the pressure reducer to the gas tubing (16).
   6. Open the gas-flow control (17) until a gas flow of about 1.1 (corresponding to about 5 mbar l/s) is shown.
   7. Flush the gas tubing for about 10 minutes to remove residual gases from the tubing.
   8. Close the valve that connects the pressure reducer to the gas tubing (16).
   9. Wait a few minutes until the He is removed from the gas tubing.
   10. (optional) For highest purity of the buffer gas, fill the cryo-trap (18) with liquid nitrogen.
   11. Set the gate valve (7) between the buffer gas cell and its turbo molecular pump to automatic operation and close the valve via the user interface (5).
   12. Open the valve that connects the pressure reducer to the gas tubing (16).
       NOTE: The buffer-gas stopping cell is now filled with ca. 30 mbar of He gas. In this way the RFQ and QMS pressures are raised to 10^{-4} mbar and 10^{-5} mbar, respectively.
   13. Adjust the rotary speed of the turbo-molecular pump of the extraction-RFQ vacuum chamber (9) to 50% in order to set an ambient pressure of about 10^{-2} mbar.

4. **Apply the electric guiding fields for continuous ion extraction**
   1. Apply a DC potential to the 233-uranium α source (1) of 39 V in continuous mode via a customized DC voltage supply (19).
   2. Apply a DC potential gradient of 4 V/cm (ranging from 35 V to 3 V) via a DC power supply (20) and a voltage offset of 3 V via a 24 channel DC offset supply (21) to the 50-fold segmented funnel ring-electrode system. All voltages are controlled with the computer-based user interface (5).
   3. Apply a DC potential of typically 2 V to the extraction nozzle electrode (22) with the help of the same computer-based user interface (5).
   4. Apply a DC potential gradient to the 12-fold segmented extraction-RFQ (27).
      NOTE: The voltage of each segment can be applied individually with the help of the computer-based user interface (5) via the 24 channel DC offset supply (21). A voltage of 1.8 V is applied to the segment closest to the extraction nozzle. The voltages of the subsequent segments are then stepwise decreased by 0.2 V, resulting in a voltage of 0 V applied to the 10th RFQ segment. This corresponds to a DC gradient of 0.1 V/cm. In case of intended continuous transport of the extracted ions a voltage of 0 V is applied to the 11th and 12th RFQ segments. For this purpose the DC voltage supply of the 12^{th} RFQ segment (23) is left at 0 V and the customized trigger module (24) is set to continuous operational mode.
   5. Apply RF frequency and amplitude to the funnel ring electrode system via a function generator (25) and linear RF amplifier (26).
      NOTE: Typical values for frequency and amplitude are 850 kHz and 220 V_{pp}, respectively. The voltages can be controlled with a computer-based user interface (5). During funnel-RF voltage application, monitor the current of the funnel DC offset supply (21). In case of sparks, which can occur if buffer-gas purity is insufficient, this current will start to increase.
   6. Apply RF frequency (typically 880 kHz) and amplitude (typically 120-250 V_{pp}) to the extraction radiofrequency quadrupole (27) (extraction-RFQ) via a frequency generator (28) and two RF amplifiers (29, 30), one for the RFQ and one for the individual bunching electrode. The voltage can be controlled with the computer-based user interface (5).
   7. Apply a DC potential of -1 V to the exit electrode (31) of the extraction-RFQ via a Mesytec MHV-4 DC voltage supply (32).
   8. Apply DC offset voltages to the quadrupole mass separator (33) (QMS). The offset voltage of the QMS (center electrode and Brubaker lenses) is chosen to be -2 V via customized DC offset modules (34,35).
   9. Start the quadrupole mass separator (33) QMS by switching on the QMS function generator (36), the RF amplifier (37) and starting the QMS user-interface (38). In the QMS user interface the mass-over-charge ratio of the selected ion species is inserted (typically 76 u/e or 114.5 u/e, for the extraction of Th^{3+} or Th^{2+}, respectively). Also the QMS acceptance (typically 1 to 2 u/e) and the RF frequency (typically 825 kHz) is inserted.
      NOTE: The Labview program will automatically apply and control the RF amplitude and the DC potentials required for ion selection. The required RF amplitudes range from 600 to 1500 V_{pp} and the DC potentials range from 50 V to 120 V. The DC potentials for mass separation are generated by a customized DC module (39). A feedback-loop is implemented for RF and DC voltage stabilization.
   10. Apply DC potential to the focusing triodic electrode structure (40) behind the QMS (-2 V/- 62 V/-22 V) via the Mesytec 4 channel (MHV-4) voltage supply module (32).

5. **Probe the ion extraction and tune the QMS**
   1. Apply an attractive surface potential of -1000 V to the front plate of the double-plate (chevron geometry) microchannel-plate detector (41) (MCP) via a high voltage (HV)-module (42).
   2. Apply a potential of +900 V to the back side of the second MCP plate via a HV-module (43).
   3. Apply a potential of +5,000 V to the phosphor screen (44) placed behind the MCP detector via a HV-module (45).
   4. Switch on the CCD camera (46) behind the phosphor screen and configure the exposure parameters of the CCD camera in the corresponding graphical user interface on the data acquisition PC (47).
      NOTE: The CCD camera is placed in a light-tight housing (48) to cover the detection from ambient light. In case that the extraction is running properly and ions are passing through the QMS a strong signal should be visible on the phosphor screen caused by the ionic impact of the extracted ions. This signal is now monitored by the CCD camera.
   5. Perform a mass scan to probe the signal shape and accordingly tune the QMS to extract the desired ion species.
      Note: This is an iterative procedure carried out with the help of the QMS user interface (38). Select a desired mass-over-charge ratio (typically 114.5 u/e for $^{229}Th^{2+}$) and the QMS resolving power (typically 1 u/e), then probe the ionic impact signal via the CCD camera. Shift the selected mass in 0.5 u/e steps until a signal is observed. As soon as a signal is observed, probe if also the $^{233}U^{2+}$ signal is observable by shifting the mass-over-charge-ratio by 2 u/e to higher masses. If also this signal is observed, probe if the signals can be

separated. If this is not the case, adapt the QMS resolving power until the $^{229}Th^{2+}$ and $^{233}U^{2+}$ signals can clearly be distinguished. Then set the QMS to extract only the $^{229}Th^{2+}$ ion species.

6. **Detection of the isomeric decay**
    1. Switch off the QMS pressure sensor (49) via the pressure sensor control unit (50) in order to reduce background from ionized helium and light produced by the sensor.
    2. Adjust the QMS parameters to extract the Th^{2+} or Th^{3+} ion species for isomeric decay detection.
    3. Reduce the surface potential of the front plate of the MCP detector (41) to -25 V via (42) in order to avoid detecting the signal from electrons originating directly from the ionic impact of impinging ions. In this way a 'soft landing' of the $^{229(m)}Th$ ions on the MCP surface is achieved prior to the isomeric decay.
    4. Apply an accelerating potential of typically +1,900 V to the second MCP plate for optimum electron amplification via (43).
    5. Apply an accelerating potential of typically +6,000 V to the phosphor screen placed behind the MCP detector via (45).
    NOTE: The actually applied voltages will depend on the MCP performance.
    6. Start the acquisition sequence of CCD images and store the data on disk via the camera user-interface (47).
    7. Use Matlab programs for image evaluation and post-processing.
    NOTE: A description of the programs and how they are used can be found in Ref.[35] Appendix B.3. Raw data of image frames as well as the programs used for evaluation have been made available online at DOI 10.5281/zenodo.1037981.

2. Measurement of the ^{229m} Th Half-Life (Re-arrangement of the Setup)

1. **Shut down and venting of the system.**
    1. Power off the high voltages of the MCP detection system (42,43,45), the QMS (37,38), the Funnel system (25,26) and extraction RFQ (28,29,30).
    2. (Optional) Power off all remaining DC voltages.
    3. Manually close the He supply system (valves 14 and 16) and wait until the pressure of the buffer-gas stopping cell is reduced to below 2 mbar.
    4. Open the gate valve that connects the turbo pump to the buffer-gas stopping cell (7) via the user interface (5) and wait until the He is fully removed from the system.
    5. Close valve (17) of the gas supply line and switch off the gas purifier (13).
    6. Set the gate valve (7) to manual operation in order to hinder it from closing when the system is vented with dry nitrogen.
    7. Close the three valves that connect the turbo pumps with the roughing pump (6) and power down the three turbo pumps (8,9,10).
    8. Switch on the QMS pressure sensor (49).
    9. Wait until the rotation speed of the turbo pumps is reduced to significantly below 100 Hz as monitored on the user interface (5).
    10. Fill the dewar (51) with liquid nitrogen and open the venting valve (52) slowly. Wait several minutes until the system is completely vented with dry nitrogen.
    NOTE: Alternatively, dry nitrogen from a gas cylinder could be used. But in this case, care has to be taken that no overpressure would occur (*e.g.,* by inserting an overpressure valve or rupture disk). The use of air is also an alternative but will lead to slightly longer evacuation times due to the humidity.
    11. Close the venting valve (52).

2. **Replace the MCP with phosphor screen (41,44) by a small single-anode MCP detector (53)**
    1. Disconnect and remove the CCD camera (46) together with the light-tight housing (48).
    2. Disconnect the MCP detector with phosphor screen (41,44).
    3. Open the vacuum flange that connects the MCP and phosphor screen with the vacuum chamber.
    4. Place the single-anode MCP (53) with a few mm distance behind the exit of the triode extraction system (40) and connect the three wires that connect the front plate (42), back plate (43) and the anode of the MCP (54) with the electric feedthroughs.
    5. Close the vacuum chamber, the system is now ready for evacuation and bake out.
    6. Provide the external wiring of the single anode MCP to the HV modules and the read-out system.

3. **Evacuation of the system and bake out**
    1. Evacuate the vacuum system by following the steps 1.2.1 to 1.2.3.
    2. Follow the bake-out procedure of steps 1.2.4 to 1.2.8.

4. **Preparation of the gas-tubing and supply of ultra-pure He**
    1. Follow the steps 1.3.1 to 1.3.12.
    NOTE: For bunched mode operation we typically operate the RFQ turbo-pump at 100 % rotation speed, resulting in a pressure in the 10^{-4} mbar range.

5. **Apply the electric guidance fields for ion bunching**
    1. Apply a DC potential of 69 V to the 233-uranium α source (1) via the customized DC voltage supply (19).
    2. Apply a DC potential gradient of 4 V/cm (ranging from 65 V to 33 V) via the DC power supply (20) and a voltage offset of 33 V via the 24 channel DC offset supply (21) to the 50-fold segmented funnel ring-electrode system. All voltages are controlled with the computer-based user interface (5).
    3. Apply a DC potential of 32 V to the extraction nozzle electrode (22) with the help of the same computer-based user interface (5).
    4. Apply a DC potential gradient to the 12-fold segmented extraction-RFQ.
    NOTE: The voltage of each segment can be applied individually with the help of the computer-based user interface (5) via the 24 channel DC offset supply (21). A voltage of 31.8 V is applied to the segment closest to the extraction nozzle. The voltages of the subsequent segments are then stepwise decreased by 0.2 V, resulting in a voltage of 30 V applied to the 10th RFQ segment. This corresponds to a DC gradient of 0.1 V/cm. In case of creation of a bunched beam the ions are stored and cooled in the 11th electrode.

Therefore, the 11th electrode is set to 25 V and the last RFQ segment is raised to 44 V via the DC voltage supply (23) to accumulate ions in the local potential bucket before releasing the ion bunch by lowering the last electrode segment to 0 V within a microsecond, triggered by a customized trigger module (24).

5. Set the trigger module (24) to bunch mode. The trigger module allows an adjustment of the trigger rate and timing. Typically, 10 Hz is chosen as the trigger rate.
6. Apply the remaining voltages to the system, following steps 1.4.5 to 1.4.10.

6. **Probe the ion extraction and tune the QMS**
   1. Switch off the QMS pressure sensor (49) via the pressure sensor control unit (50) in order to reduce background from ionized helium and light produced by the sensor.
   2. Apply an attractive surface potential of -2,000 V to the front plate of the single anode MCP (52) via a HV-module (42).
   3. Apply a potential of -100 V to the back side of the MCP. The MCP anode is set to ground.
   4. Switch on the 12 V power supply module (55) for the MCP preamplifier (56).
      NOTE: Single ions impinging on the MCP detector are now counted with the help of the combination of the preamplifier (56), an amplifier (57) and a constant fraction discriminator (CFD) (58). The CFD signal is send to a data acquisition (DAQ) card of the PC used for QMS control and can be monitored via the QMS user interface (38).
   5. Perform a mass scan to probe the signal shape and accordingly tune the QMS to extract the desired ion species.
      NOTE: This is done with the help of the QMS user Interface (38). For this purpose, an initial and a final mass-over-charge ratio is set (*e.g.,* 110 u/e to 120 u/e for the $^{229}Th^{2+}$ mass-range), as well as the resolving power (*e.g.,* 1 u/e) and the integration time (5 s) per scan step and the mass scan is started by pressing the scan button. In case that the extraction is running properly and ions are passing the QMS, strong signals of thorium and uranium will be visible caused by the ionic impact of the extracted ions.

7. **Lifetime measurement**
   1. Adjust the QMS parameters to extract the Th^{2+} or Th^{3+} ion species for isomeric decay detection.
   2. Reduce the surface potential of the front plate of the MCP detector (52) to -25 V via (42) in order to reduce the ionic impact signal.
   3. Apply an accelerating potential of typically +1,900 V to the second MCP plate for optimum electron amplification via (43).
   4. Apply an accelerating potential of typically +2,100 V to the MCP anode via (53).
   5. Start the data acquisition via a microchannel scaler (59).
      NOTE: The preamplifier (56) and the microchannel scaler (59) allow for time resolved read-out of the MCP detector. The ion bunches and the microchannel scaler are both triggered by the trigger module (24). The scaler signal is obtained via a Labview user interface (60). An exponential decay tail of about 10 microseconds lifetime becomes visible after the ion bunches, corresponding to the thorium isomeric decay.

Representative Results

The method described before allowed for the extraction of α decay products from a ^{233}U source placed inside a buffer-gas stopping cell, operated at ca. 30 mbar ultra-pure helium gas at room temperature. For the first time up to triply charged ions could be extracted from such a device with high efficiency[29]. **Figure 3a** displays the mass spectrum of ions extracted from the buffer-gas cell, showing three groups of ^{233}U α-decay products (plus accompanying contaminant adducts) in singly, doubly and triply charged ionic states. Noteworthy is the dominance of $^{229}Th^{3+}$ extraction compared to $^{233}U^{3+}$, while both species are extracted with about equal intensity when being doubly charged. This fact was used for comparative measurements with ^{233}U ions, which allowed the exclusion of any ionic impact as signal origin.

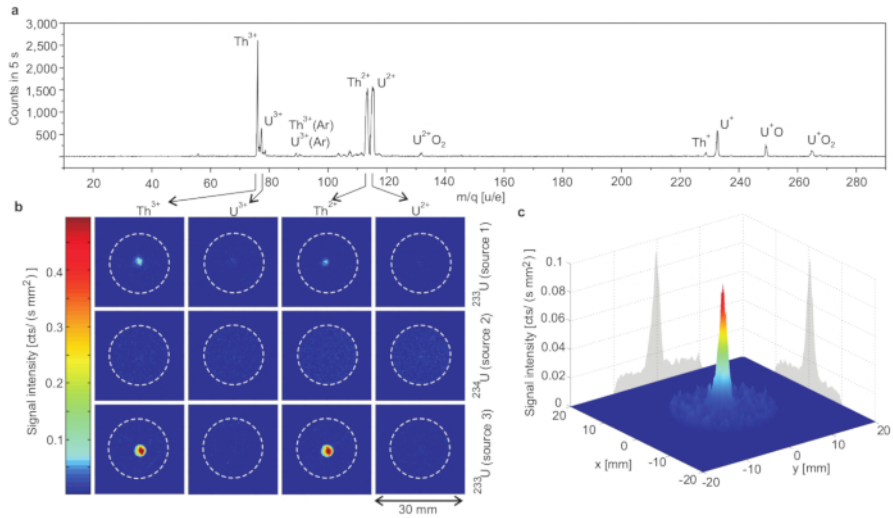

Figure 3: Identification of the direct decay of the 229-thorium isomer. a) Complete mass scan performed with the ^{233}U source 1[29]. Units are given as atomic mass (u) over electric charge (e). b) Comparison of MCP signals obtained during accumulation of thorium and uranium in the 2+ and 3+ charge states (as indicated by the arrows linking to the mass scan). ^{233}U and ^{234}U sources were used (the source number is given on the right-hand side of each row). Each image corresponds to an individual measurement of 2,000 s integration time (20 mm diameter aperture indicated by the dashed circle). Measurements were performed at -25 V MCP surface voltage in order to guarantee soft landing of the ions. c) Signal of the ^{229}Th isomeric decay obtained during ^{229}Th^{3+} extraction with source 1. A signal area diameter of about 2 mm (FWHM) is achieved. The obtained maximum signal intensity is 0.08 counts/(s mm^2) at a background rate of about 0.01 counts /(s mm^2). With kind permission of Springer Research [11]. Please click here to view a larger version of this figure.

After transport, cooling and mass separation, the ion beam impinges onto the surface of a microchannel-plate detector, where a low attractive surface potential ensures the suppression of ionic impact signals and leaves only electrons arising from the Internal Conversion (IC) decay channel of the ^{229m}Th isomer to be multiplied in the strong electric field of the detector plate channels. The resulting MCP signals as obtained for three different uranium sources are displayed in **Figure 3b**. The ion species of doubly or triply charged ions which was selected with the help of the quadrupole mass separator in each individual measurement is indicated by the arrows from the upper panel. Shown are pictures acquired with the CCD camera behind the phosphor screen, onto which the electrons from the MCP were accelerated. The field of view of the CCD camera is indicated by the dashed circles for triply (first two columns) and doubly charged (last two columns) ^{229}Th and ^{233}U ions, respectively. The upper row represents the result obtained for a small-area ^{233}U source (ca. 1000 extracted ^{229}Th^{3+} ions per second, source 1), while the bottom row shows the same for a stronger source with ca. 10,000 extracted ^{229}Th^{3+} ions per second (source 3). It is obvious that in both cases a clear signal is obtained for ^{229}Th, while no indication of an electron signal is observed for ^{233}U 11. In order to prove that this signal indeed originates from a nuclear deexcitation and not from an atomic shell process, the middle row shows the resulting camera image when using a ^{234}U source, where the α decay populates the neighboring isotope ^{230}Th, with a comparable electronic, yet different nuclear structure. As expected for ^{230}Th, no indication of a conversion electron signal is found in any of the cases studied. So the strong signal, displayed in **Figure 3c** with excellent signal-to-background ratio, is clearly correlated with the decay of ^{229m}Th.

Additional verification measurements to support this interpretation are shown in **Figure 4**. They show two measurements to give further evidence that the registered electron signals indeed originate from the decay of the nuclear isomer: in **Figure 4a** it is shown that the attractive surface potential of the MCP detector was varied from -100 V (favoring the occurrence of electrons from ionic impact) down to 0 V, comparing the count rates registered with the MCP for extracted ^{229}Th^{2+} (red) and ^{233}U^{2+} ions (blue). Clearly the count rate drops down to zero for ^{233}U^{2+} when realizing a 'soft landing' of the incoming ions with a surface voltage below ca. -40 V, while a considerable count rate remains for ^{229}Th^{2+} until the threshold of 0 V. In **Figure 4b**, the blue curve shows the electron count rate registered for extracted ions after strong acceleration towards the MCP detector surface with -2000 V. Ionic impact of ^{233}U^{2+} and ^{229}Th^{2+} ions is observed with about equal intensity, as already shown for doubly charged ions in the extracted mass spectrum of **Figure 3a**. The red curve shows the same scenario, however now for a 'soft landing' of incoming ions with -25 V MCP surface potential. No indication of the ionic impact signal of ^{233}U^{2+} is visible any more, while for ^{229}Th^{2+} a signal remains, originating from the isomeric internal conversion decay[11].

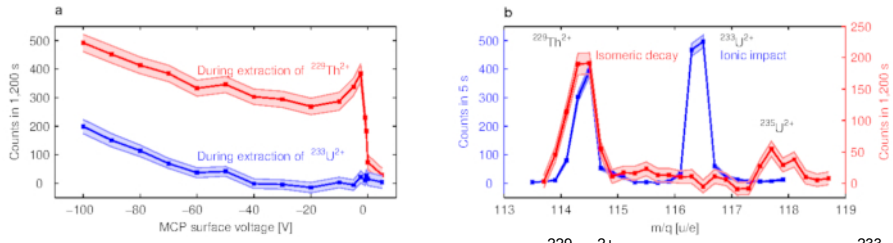

Figure 4: Isomer decay verification measurements. a) $^{229}Th^{2+}$ signal (red) compared to $^{233}U^{2+}$ (blue) as a function of the MCP surface voltage. Errors are indicated by shaded bands. b) Signal of extracted ions as a function of the mass-to-charge ratio behind the QMS for MCP surface voltages of -25 V (isomer decay, red) and -2,000 V (ion impact, blue). Note the different integration times and axis scales. In addition to the signal at 114.5 u/e (corresponding to $^{229}Th^{2+}$), a further signal at 117.5 u/e occurs, which originates from the isomeric decay of ^{235}U. With kind permission of Springer Research[11]. Please click here to view a larger version of this figure.

Thus, it can be unambiguously proven (together with additional arguments given in Ref. [11]) that the signal observed in **Figure 4** originates from the isomeric decay of ^{229m}Th and represents the first direct identification of the deexcitation of this elusive isomer.

Subsequently the segmented extraction-RFQ was operated as a linear Paul trap to create a bunched ion beam, thus allowing for lifetime measurements of the thorium isomer. Since our room-temperature high vacuum does not allow for sufficiently long storage times to investigate the expected radiative lifetime of up to 10^4 seconds, only a lower limit of $t_{1/2} > 1$ minute could be derived for charged ^{229m}Th ions, limited by the maximum achievable ion storage time in the linear Paul trap[11]. However, using the same detection strategy as applied before for the identification of the isomer decay after neutralization of the thorium ions on the surface of an MCP detector, the expected much shorter lifetime for neutral ^{229m}Th atoms undergoing internal conversion decay provides access to lifetime information[12]. **Figure 5a** shows the expected shape of the decay time spectrum as simulated for an ion bunch with a pulse width of 10 µs. While the red curve indicates the ionic impact signal and the signal from an exponential decay with 7 µs half-life is represented by the gray curve with a long decay tail, the expected signal from the decay of the thorium isomer, comprised of both the ionic impact and the exponential isomeric decay, is illustrated by the blue curve. **Figure 5b** displays the outcome of the corresponding measurement for $^{233}U^{3+}$ (red) and $^{229}Th^{3+}$ (blue), respectively. While uranium ions only exhibit their ionic impact signal, for 229-thorium clearly the expected decay tail of the isomer decay can be observed[12].

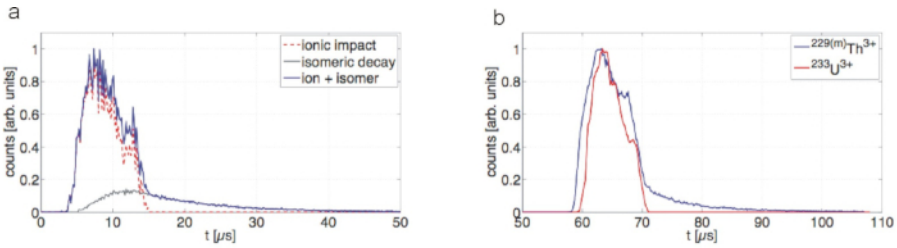

Figure 5: Simulated and measured temporal ion impact and decay characteristics. a) Simulation of the isomer decay time characteristics of ^{229}Th bunches. The simulation is based on a measured bunch shape and the assumption that 2 % of the ^{229}Th ions are in the isomeric state with a half-life of 7 µs after neutralization. The electron detection efficiency is assumed to be 25 times larger than the ion detection efficiency. b) Measurement of the isomeric decay with a bunched $^{229(m)}Th^{3+}$ ion beam (blue). A comparative measurement with $^{233}U^{3+}$ is shown in red. With kind permission of the American Physical Society[12]. Please click here to view a larger version of this figure.

Fitting the decay tail with an exponential (corresponding to a linear fit to the logarithmic representation in **Figure 6**) finally results in a half-life of the neutral ^{229m}Th isomer of 7(1) µs[12]. This value nicely agrees with the theoretically expected lifetime reduction by nine orders of magnitude from the ca. 10^4 seconds in case of the charged isomer due to the large conversion coefficient of $\alpha_{IC} \sim 10^9$ [37].

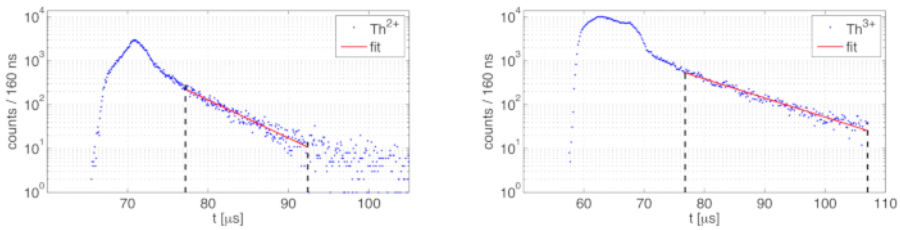

Figure 6: Fit to ^{229m}Th decay curve. Logarithmic plot of the temporal decay characteristics for $^{229(m)}Th^{2+}$ ions (a) and $^{229}(m)Th^{3+}$ ions (b) together with a fit curve applied to extract the isomeric half-life of ^{229m}Th after charge recombination on the MCP detector surface. With kind permission of the American Physical Society[12]. Please click here to view a larger version of this figure.

Discussion

The range of recoiling α decay daughter nuclei in uranium amounts to only about 16 nm. In order to achieve a high efficiency of the source for α-recoil ions for a given source activity, it is mandatory to limit the source material thickness to this range. The α recoil extraction efficiency is strongly affected by the cleanliness of the buffer-gas cell. Contaminations of the stopping gas will lead to charge exchange or molecule formation. Therefore, the gas cell itself has to be built according to ultra-high vacuum standards, in particular to allow for a baking of the cell and

avoiding any organic materials inside. The stopping gas has to be purified according to technical state-of-the-art, starting from highest-grade gas purity assisted by catalytic purification and delivery to the gas cell via an ultra-clean gas-supply line, partially surrounded by a cryogenic trap to freeze out impurities. In general, careful alignment of the central axis of the complete setup to the position of the gas cell extraction nozzle is essential for achieving a high transport and detection efficiency[29].

Step 1.4.5 is the most critical of the protocol. For efficient ion extraction a high RF amplitude has to be applied to the funnel ring electrode. However, if the amplitude is chosen too high, sparks in the gas cell will occur. The maximum achievable RF voltage amplitude depends critically on the purity of the buffer gas. A successful application of voltage is monitored via the current of the funnel offset voltage. This current will increase in the case of sparks. If sparks have occurred, the bake-out procedure has to be repeated in order to guarantee highest ion extraction efficiency.

A further critical point is the application of the high voltages to the MCP detector (steps 1.6.2-1.6.4). Field emissions can occur on the MCP, leading to the emission of electrons which can lead to artefactual signals.

Optimum ion extraction and (cooled and mass purified) transport towards the detection unit requires careful alignment of the central optical axis. The availability of an optical alignment system (alignment laser or theodolite) is essential. The efficient ion transport through the extraction RFQ and the QMS requires a continuous stabilization of the radio-frequency amplitudes for the two opposite phases applied to each opposite pair of rods[29]. Identification of extraction or transport problems can be facilitated by an ion diagnostic realized *e.g.,* via a multichannel-plate detector placed either consecutively at different positions along the ion path during the commissioning phase of the setup, or alternatively, *e.g.,* under 90° behind the extraction RFQ with a high negative surface voltage (1-2 kV) to attract all extracted ions towards the detector.

During operation typically two problems can arise. Not all voltages are correctly applied. In this case usually no ions are extracted, and one has to find the place of not correctly applied voltage. Also, impurities are present in the helium buffer-gas. In this case the extraction efficiency for triply charged thorium ions will be drastically reduced and molecule formation occurs. In the worst case, even sparks will show up when the funnel voltage is applied. The reason for insufficient gas purity is typically a leakage in the gas supply line or a not properly closed flange of the buffer-gas stopping cell.

The described method to generate a clean beam of ions containing the energetically low-lying ^{229m}Th isomer can be applied to all comparable cases where the ion of interest can be extracted from the buffer-gas atmosphere in sizeable amounts. Cleanliness of the gas-cell and buffer gas is mandatory, thus the amount of remaining gas impurities is a limitation to the sensitivity of the method. While the employed microchannel-plate detector (MCP) is based on the detection of electrons, as exploited here for the registration of low-energy conversion electrons, this case already lies at the low-energy border of the efficiency curve for MCPs[38], while for higher energies the method would significantly gain in detection efficiency.

So far, the described method has provided the only reported direct and unambiguous identification of the de-excitation of the thorium isomer. Alternatively, vacuum ultra-violet (VUV)-transparent crystals (with large bandgaps, exceeding the assumed excitation energy of the isomer) are doped with ^{229}Th. The goal is to place ^{229}Th ions in high (4^+) charge state of crystal lattice positions, inhibit de-excitation by the large band gap and aim at an excitation of the isomer using X- rays from synchrotron light sources. Despite the elegant concept of this approach, so far no VUV fluorescence could be observed in a series of experiments reported by several groups worldwide[39,40,41,42,43]. The same holds for a class of experiments that aims to realize the nuclear excitation of the isomer via the electron shell of ^{229}Th, using a so-called electron-bridge transition. Here a resonant coupling between an electron shell transition and the nuclear isomer should allow for a more efficient isomer population[44,45]. Other experiments that aim for the investigation of the isomeric properties are based on microcalorimetry[46] or the observation of the hyperfine-shift in the atomic shell[47]. Very recently another method to excite the isomer in a laser-induced plasma was reported[48] and is subject to scientific discussion within the community.

The discovery of the internal conversion decay channel of the thorium isomer[11] and the determination of the corresponding half-life of neutral ^{229m}Th (7(1) µs)[12] can be exploited in the future to realize a first all-optical excitation with a pulsed, tunable VUV laser based on already existing technology. Thus the present paradigm that this would require much better knowledge of the excitation energy and a corresponding customized laser development can be circumvented. In contrast, exploiting the knowledge of internal conversion electron emission, gating the detection of conversion electrons with the laser pulse will provide a high signal-to-background ratio, while allowing for a scan of 1 eV of excitation energy in less than 3 days[49].Moreover, a determination of the excitation energy of the isomer, still being work in progress, can be based on the described method of generating the ^{229m}Th beam by sending IC decay electrons into a magnetic-bottle electron spectrometer with retarding field electrode grids[50]. The same technique will also allow to determine the isomeric lifetime for different chemical environments (*e.g.,* on large band-gap materials like CaF_2 or frozen argon) or in $^{229}Th^+$ as well as in the free, neutral atom.

The described method of generating an isotopically pure thorium ion beam of 3+ charge state can be used as a tool to provide thorium ions for future laser-spectroscopy experiments. In this case the ion beam can be used to load a Paul trap in a stable and efficient way. So far, the only alternative method is to produce $^{229}Th^{3+}$ by laser ablation from a solid target. This, however, requires high laser intensities and a large quantity of ^{229}Th, which is an expensive radioactive material and leads to the contamination of used vacuum components. For this reason, the described method can be of significant advantage when it comes to nuclear laser spectroscopy experiments. A first application of this type has already been published[51].

Disclosures

The authors have nothing to disclose.

Acknowledgments

This work was supported by the European Union's Horizon 2020 research and innovation program under Grant Agreement No. 664732 "nuClock", by DFG grant Th956/3-1, and by the LMU department of Medical Physics via the Maier-Leibnitz-Laboratory.

References

1. Reich, C.W., Helmer, R.G., Energy separation of the doublet of intrinsic states at the ground state of ^{229}Th. *Physical Review Letters.* **64**, 271-273 (1990).
2. Reich, C.W., Helmer, R.G., An excited state of ^{229}Th at 3.5 eV. *Physical Review C.* **49**, 1845 - 1858 (1994).
3. Guimaraes-Filho, Z.O., Helene, O., Energy of the $3/2^+$ state of ^{229}Th reexamined. *Physical Review C.* **71**, 044303 (2005).
4. Beck, B.R. *et al.* Energy splitting of the ground-state doublet in the nucleus ^{229}Th. *Physical Review Letters.* **98**, 142501 (2007).
5. Beck, B.R. *et al.* Improved value for the energy splitting of the ground-state doublet in the nucleus ^{229}Th. *Proceedings of the 12th International Conference on Nuclear Reaction Mechanisms.* Varenna, 2009, edited by F. Cerutti and A. Ferrari, *LLNL-PROC-415170* (2009).
6. Tkalya, E.V., Proposal for a nuclear gamma-ray laser of optical range. *Physical Review Letters.* **106**, 162501 (2011).
7. Raeder, S. *et al.* Resonance ionization spectroscopy of thorium isotopes-towards a laser spectroscopic identification of the low-lying 7.6 eV isomer of ^{229}Th. *NJ. Physics. B.* **44**, 165005 (2011).
8. Peik, E., Tamm, C., Nuclear laser spectroscopy of the 3.5 eV transition in ^{229}Th. *European Physical Letters.* **61**, 181-186 (2003).
9. Campbell, C.J., Radnaev, A.G., Kuzmich, A., Dzuba, V.A., Flambaum, V.V., Derevianko, A Single-Ion nuclear clock for metrology at the 19th decimal place. *Physical Review Letters.* **108**, 120802 (2012).
10. Kroger, L.A., Reich, C.W., Features of the low energy level scheme of ^{229}Th as observed in the α decay of ^{233}U. *Nuclear Physics A .* **259**, 29-60 (1976).
11. v.d. Wense, L. et al. Direct detection of the Thorium-229 nuclear clock transition. *Nature.* **533**, 47-51 (2016).
12. Seiferle, B., v.d. Wense, L., Thirolf, P.G. Lifetime measurement of the ^{229}Th nuclear isomer. *Physical Review Letters .***118**, 042501 (2017).
13. Nicholson, T.L. *et al.* Systematic evaluation of an atomic clock at $2\cdot10^{-18}$ total uncertainty. *Nature Communications.* **6**, 7896 (2015).
14. Flury, J., Relativistic geodesy. *Journal of Physics - Conference Series.* **723**, 012051 (2016).
15. Ludlow, A.D., Boyd, M.M., Ye, J., Peik, E., Schmidt, P.O. Optical atomic clocks. *Reviews of Modern Physics.* **87**, 637-701 (2015).
16. Derevianko, A., Pospelov, M., Hunting for topological dark matter with atomic clocks. *Nature Physics.* **10**, 933-936 (2014).
17. Uzan, J.P., The fundamental constants and their variation: observational and theoretical status. *Review of Modern Physics.* **75**, 403-455 (2003).
18. Flambaum, V.V., Enhanced effect of temporal variation of the fine structure constant and the strong interaction in ^{229}Th. *Physical Review Letters.* **97**, 092502 (2006).
19. He, X., Ren, Z. ,Temporal variation of the fine structure constant and the strong interaction parameter in the ^{229}Th transition. *Nuclear Physics A.* **806**, 117-123 (2008).
20. Litvinova, E., Feldmeier, H., Dobaczewski, J., Flambaum, V., Nuclear structure of lowest ^{229}Th states and time dependent fundamental constants. *Physical Review C.* **79,** 064303 (2009).
21. Flambaum, V.V., Wiringa, R.B., Enhanced effect of quark mass variation in Th229 and limits from Oklo data. *Physical Review C.* **79**, 034302 (2009).
22. Rellergert, W.G., *et al.* Constraining the evolution of the fundamental constants with a solid-state optical frequency reference based on the ^{229}Th nucleus. *Physical Review Letters.* **104**, 200802 (2010).
23. Hayes, A.C., Friar, J.L., Sensitivity of nuclear transition frequencies to temporal variation of the fine structure constant or the strong interaction. *Physics Letters B.* **650**, 229-232 (2007).
24. Berengut, J.C., Dzuba, V.A., Flambaum, V.V., Porsev, S.G. Proposed experimental method to determine a sensitivity of splitting between ground and 7.6 eV isomeric states in ^{229}Th. *Physical Review Letters .* **102**, 210808 (2009).
25. Flambaum, V.V., Auerbach, N., Dmitriev, V.F., Coulomb energy contribution to the excitation energy in ^{229}Th and enhanced effect of α variation. *Europhysics Letters.* **85**, 50005 (2009).
26. Porsev, S.G., Flambaum, V.V., Effect of atomic electrons on the 7.6 eV nuclear transition in $^{229m}Th^{3+}$. *Physical Review A .* **81**, 032504 (2010).
27. Godun, R.M., *et al.*, Frequency ratio of two optical clock transitions in $^{171}Yb^+$ and constraints on the time variation of fundamental constants. *Physical Review Letters.* **113**, 210801 (2014).
28. v.d. Wense, L., Thirolf, P.G., Kalb, D., Laatiaoui, M., Towards a direct transition energy measurement of the lowest nuclear excitation in ^{229m}Th. *Journal of Instrumentation.* **8**, P03005 (2013).
29. v.d. Wense, L., Seiferle, B., Laatiaoui, M., Thirolf, P.G., Determination of the extraction efficiency for ^{233}U source recoil ions from the MLL buffer-gas stopping cell. *European Physical Journal A.* **51**, 29 (2015).
30. Neumayr, J.B., *The buffer-gas cell and extraction RFQ for SHIPTRAP.* PhD Thesis, LMU Munich, Germany (2004).
31. Neumayr, J.B. et al. The ion-catcher device for SHIPTRAP. *Nuclear Instruments and Methods in Physics Research Section B.* **244**, 489-500 (2006).
32. Neumayr, J.B. et al. Performance of the MLL-Ion catcher. *Review of Scientific Instruments.* **77**, 065109 (2006).
33. Haettner, E., *A novel radio frequency quadrupole system for SHIPTRAP & New mass measurements of rp nuclides.* PhD Thesis, University of Giessen, Germany (2011).
34. Haettner, E. et al. A versatile triple radiofrequency quadrupole system for cooling, mass separation and bunching of exotic nuclei. *Nuclear Instruments and Methods in Physics Research A.* **880**, 138-151 (2018).
35. v.d. Wense, L., On the direct detection of ^{229m}Th. *Springer Theses, Springer international publishing, ISBN 978-3-319-70460-9.* (2018).
36. Eberhardt, K. et al. Actinide targets for fundamental research in nuclear physics. *AIP Conference Proceeding 1962s.* **030009** (2018).
37. Karpeshin, F.F., Trzhaskovskaya, M.B., Impact of the electron environment on the lifetime of the 229Thm low-lying isomer. *Physical Review C .* **76**, 054313 (2007).
38. Gorugantu, R.R., Wilson, W.G., Relative electron detection efficiency of microchannel plates from 0-3 keV. *Review of Scientific Instruments .* **55**, 2030-2033 (1984).

39. Jeet, J. et al. Results of a direct search using synchrotron radiation for the low-energy ^{229}Th nuclear isomeric transition. *Physical Review Letters* . **114**, 253001 (2015).
40. Yamaguchi, A., Kolbe, M. Kaser, H., Reichel, T., Gottwald, A., Peik, E., Experimental search for the low-energy nuclear transition in ^{229}Th with undulator radiation. *New Journal of Physics.* **17**, 053053 (2015).
41. Stellmer, S., Schreitl, M., Schumm, T., Radioluminescence and photoluminescence of Th:CaF_2 crystals, *Scientific Reports.* **5**, 15580 (2015).
42. Stellmer, S., Schreitl, M., Kazakov, G.A., Sterba, J.H., Schumm, T., Feasibility study of measuring the ^{229}Th nuclear isomer transition with ^{233}U-doped crystals. *Physical Review C.* **94**, 014302 (2016).
43. Stellmer, S. *et al.* On an attempt to optically excite the nuclear isomer in Th-229. *arXiv:1803.09294 [physics.atom-ph].* (2018).
44. Porsev, S.G., Flambaum, V.V., Peik, E., Tamm, C., Excitation of the isomeric ^{229m}Th nuclear state via an electronic bridge process in $^{229}Th^{+}$. *Physical Review Letters.* **105**, 182501 (2010).
45. Campbell, C.J., Radnaev, A.G., Kuzmich, A.,*Wigner Crystals of* ^{229}Th for optical excitation of the nuclear isomer. *Physical Review Letters.* **106**, 223001 (2011).
46. Kazakov, G. *et al.* Prospects for measuring the ^{229}Th isomer energy using a metallic magnetic microcalorimeter. *Nuclear Instruments and Methods in Physics Research A.* **735**, 229- 239(2014).
47. Sonnenschein, V. *et al.* The search for the existence of ^{229m}Th at IGISOL. *European Physical Journal A.* **48**, 52 (2012).
48. Borisyuk, P.V. et al. Excitation energy of ^{229}Th nuclei in laser plasma: the energy and half-life of the low-lying isomeric state. *arXiv:1804.00299v1 [nucl-th]* .(2018).
49. v.d. Wense, L. et al. A laser excitation scheme for ^{229m}Th. *Physical Review Letters.* **119**, 132503 (2017).
50. Seiferle, B., v.d. Wense, L., Thirolf, P.G., Feasibility study of Internal Conversion Electron Spectroscopy of ^{229m}Th. *European Physical Journal A.* **53**, 108 (2017).
51. Thielking, J. *et al.* Laser spectroscopic characterization of the nuclear-clock isomer ^{229m}Th. *Nature.* **556**, 321-325 (2018).